

Coherence lengths and anisotropy in MgB₂ superconductor

A. Dulčić, M. Požek, and D. Paar

Department of Physics, Faculty of Science, University of Zagreb, P.O. Box 331, HR-10002 Zagreb, Croatia

Eun-Mi Choi, Hyun-Jung Kim, W. N. Kang, and Sung-Ik Lee

National Creative Research Initiative Center for Superconductivity and Department of Physics, Pohang University of Science and Technology, Pohang 790-784, Republic of Korea

(Received 26 July 2002; published 17 January 2003)

Field- and temperature-dependent microwave measurements have been carried out on MgB₂ thin film grown on Al₂O₃ substrate. The analysis reveals the mean-field coherence length ξ_{MF} in the mixed state and a temperature-independent anisotropy ratio $\gamma_{MF} = \xi_{MF}^{ab} / \xi_{MF}^c \approx 2$. At the superconducting transition, the scaling of the fluctuation conductivity yields the Ginzburg-Landau coherence length with a different anisotropy ratio $\gamma_{GL} = 2.8$, also temperature independent.

DOI: 10.1103/PhysRevB.67.020507

PACS number(s): 74.25.Op, 74.25.Nf, 74.40.+k, 74.78.Db

The recent discovery of superconductivity at 39 K in the simple binary compound MgB₂ (Ref. 1) has sparked a considerable effort in the scientific community to determine the fundamental parameters and the nature of superconductivity in this compound. Quite surprisingly, the usually simple determination of the upper critical field B_{c2} has emerged as a controversial issue. The early attempts to determine B_{c2}^c ($\mathbf{B} \parallel c$ axis), and B_{c2}^{ab} ($\mathbf{B} \parallel ab$ plane), have shown a large span of values and anisotropy ratio $\gamma = B_{c2}^{ab} / B_{c2}^c$ varying in the range 1.2–9.² One could have ascribed these discrepancies to an insufficient control of the sample preparation conditions at the early stage. However, the controversy has not been fully settled even with the improved sample quality in the recently prepared thin films and single crystals of MgB₂.^{3–12} One of the puzzling observations was that different experimental techniques often yielded strongly diverse B_{c2} values in one and the same sample. Thus, Welp *et al.*⁹ have shown that resistive onset of superconductivity in a given field, which was traditionally taken as the upper critical field, was in discord with the B_{c2}^c values obtained in the same sample by specific heat and magnetization measurements. Similar discrepancy has been observed in the results of the resistive onset and the thermal conductivity.¹² On the other hand, the onset of the diamagnetic response was found to corroborate with the zero resistance (or the onset of finite resistivity).¹¹

The common approach in these methods is to make a choice of a percentage in cutting the transition curves. The corresponding points are then taken for $B_{c2}(T)$. Alternatively, one looks for the geometrical intersection of the tangents above and below the transition. None of these choices, however, is guided by a physical law describing the transition.

In this Rapid Communication, we show that the problem of the upper critical field, and the related coherence length, is more subtle than implicitly assumed before. Our analysis is based on the physical process that defines the shape of the experimental curve, and yields unequivocally the value of B_{c2} . We find the mean-field (MF) coherence length ξ_{MF} as the radius of the vortex core in the mixed state and, separately, the Ginzburg-Landau (GL) coherence length ξ_{GL} at

the transition. The two coherence lengths are quite different in MgB₂. The anisotropy ratios are also different ($\gamma_{GL} > \gamma_{MF}$), but both turn out to be temperature independent.

The thin film of MgB₂ was grown on (1 $\bar{1}$ 02) Al₂O₃ substrate using a two-step method.^{13,14} Precursor thin film of B was deposited by pulsed laser deposition at room temperature. The B thin film was sealed together with high purity Mg into Nb tube with Ar atmosphere. The heat treatment was carried out at 900 °C for 10–30 min. The film thickness was 400 nm. X-ray diffraction indicated that the MgB₂ film has a highly c -axis oriented crystal structure normal to the substrate surface with no impurity phase observed. These films have been studied previously by dc resistivity, magnetization,^{13,14} penetration depth,¹⁵ and zero-field microwave measurements.¹⁶ These studies have supported the generally observed features of MgB₂ superconductor, anisotropy, and two-gap nature.

Microwave measurements were carried out in an elliptical cavity resonating in ${}_{e}TE_{111}$ mode at 9.3 GHz. The thin film was mounted on a sapphire sample holder and placed in the center of the cavity where the microwave electric field E_{ω} was maximum. The sample was oriented with ab plane parallel to E_{ω} . The measured quantities were the Q factor of the cavity loaded with the sample and the shift of the resonant frequency f . From the complex-frequency shift $\Delta\tilde{\omega}/\omega = \Delta f/f + i\Delta(1/2Q)$, one can obtain by inversion the complex conductivity $\tilde{\sigma} = \sigma_1 - i\sigma_2$ of the film using the cavity perturbation expression.¹⁷

Figure 1 shows the experimental results in zero magnetic field. From the imaginary part of the conductivity $\sigma_2 = 1/\mu_0\omega\lambda_L^2$, one can infer the zero-temperature London penetration depth $\lambda_L(0) = 79$ nm in our film. With this value, and the shape of σ_2 , this film is found to be between the clean and the dirty limit, closer to the latter.¹⁸

Here we focus on the effects of the applied magnetic field in the superconducting state. Figure 2 shows the field dependences ($\mathbf{B} \parallel c$) of the complex-frequency shift at various temperatures. By inversion of these data points, one can obtain the field-dependent complex conductivity at each given temperature. Theoretically, the response of the superconductor in

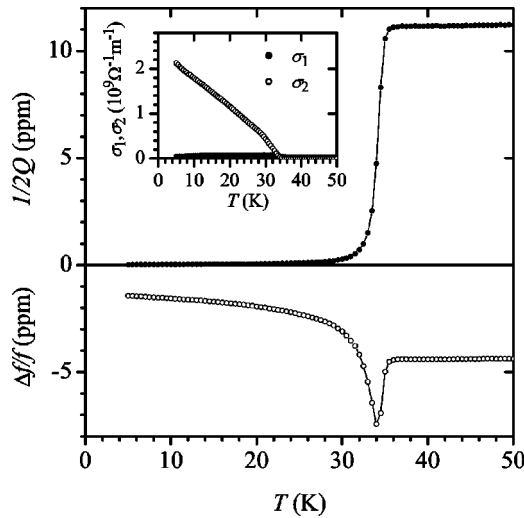


FIG. 1. Plots of imaginary and real parts of the complex-frequency shift in MgB_2 thin film in zero magnetic field. Inset shows the corresponding conductivities.

the mixed state to an oscillating electric field E_ω is given by an effective complex conductivity¹⁹

$$\frac{1}{\tilde{\sigma}_{\text{eff}}} = \frac{1 - \frac{B/B_{c2}}{1 - i(\omega_0/\omega)}}{\left(1 - \frac{B}{B_{c2}}\right)(\sigma_1 - i\sigma_2) + \frac{B}{B_{c2}}\sigma_n} + \frac{1}{\sigma_n} \frac{B/B_{c2}}{1 - i(\omega_0/\omega)}. \quad (1)$$

The first term is due to the microwave current outside the vortex cores, and the second due to the normal current in the cores of the oscillating vortices. The meaning of the fraction B/B_{c2} in Eq. (1) is the volume fraction of the sample taken

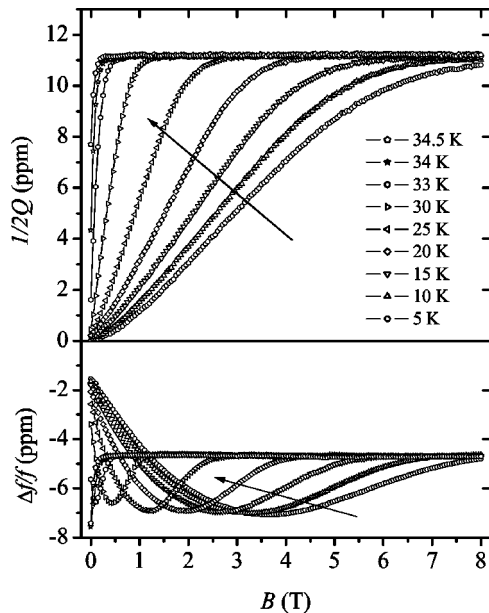


FIG. 2. Magnetic-field dependences of the complex-frequency shift in MgB_2 thin film for $\mathbf{B} \parallel c$. The arrows indicate increasing temperatures.

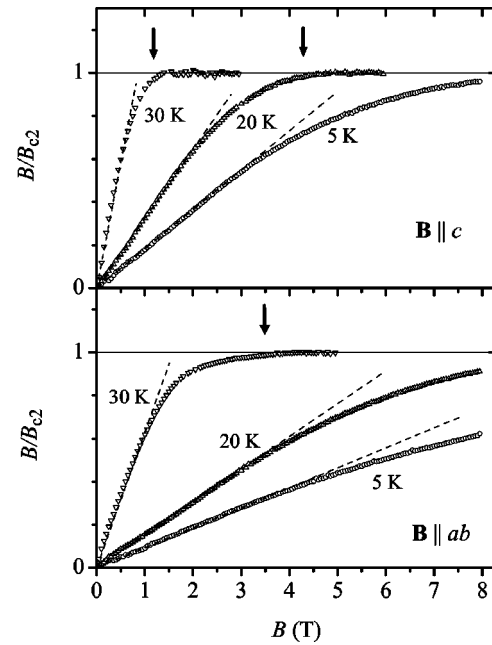


FIG. 3. Variations of the volume fraction of the normal electrons. The dashed lines mark the low-field linear segments of the curves wherefrom B_{c2}^{MF} can be determined. The arrows indicate the B_{c2}^{LLL} values obtained from the 3D LLL scaling of the fluctuation conductivity in Fig. 4.

by the normal vortex cores. This parameter determines the dc resistivity in the flux flow regime,²⁰ and has been used also in the microwave studies on classical superconductors.²¹ The depinning frequency ω_0 may change with field and temperature from the strongly pinned case ($\omega_0 \gg \omega$) to the flux flow limit ($\omega_0 \ll \omega$). In Eq. (1), the zero-field conductivity is $\sigma_1 - i\sigma_2$, and σ_n is the normal-state conductivity. Similar magnetic-field-dependent microwave studies have been carried out extensively on high- T_c superconductors.^{22–24}

Using the experimental field-dependent complex conductivity and Eq. (1), we have determined the values of B/B_{c2} and ω_0/ω . Figure 3 shows some of the results. One observes that each of the curves has initially a constant slope (dashed lines in Fig. 3). It defines very precisely the value of B_{c2} at a given temperature. Note that in this region the actual field B is much smaller than B_{c2} , so that the superconducting film is well in the mixed state. Hence, we determine, in fact, the mean-field coherence length ξ_{MF} as the radius of the normal vortex core ($B_{c2}^{MF} = \Phi_0/2\pi\xi_{MF}^2$, where Φ_0 is the flux quantum). The fundamental property of a vortex much below the transition to the normal state is that it contains many Landau levels as bound superconducting states.²⁰ When the field is increased so that the transition to the normal state is approached, the upper Landau levels are gradually lifted and finally only the lowest Landau level remains. The field at which this level nucleates is conventionally known as the upper critical field B_{c2} . When the transition is very sharp, B_{c2} can be determined straightforwardly from the single turning point. However, in the cases of rounded transitions, one has to consider the fluctuation conductivity and the scaling laws, which govern the physics of the transition. At high

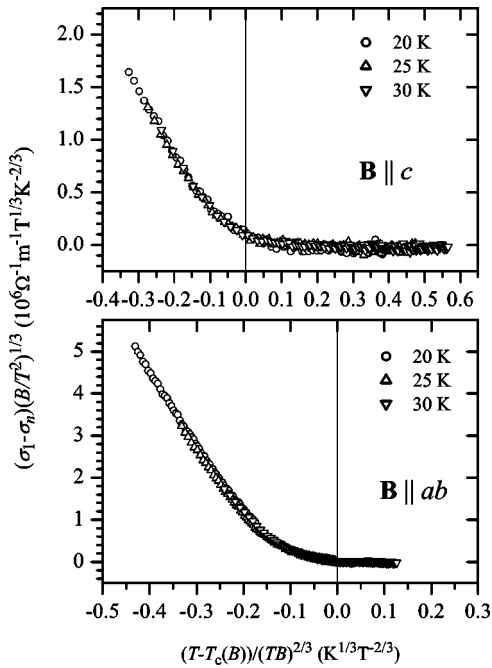


FIG. 4. 3D LLL scaling of the fluctuation conductivity $\sigma_1 - \sigma_n$.

magnetic fields, one can use the scaling law based on the lowest Landau level (LLL) scheme.²⁵ It has been used successfully in high- T_c superconductors to determine the B_{c2} line.²⁶

In Fig. 4 we show the scaling of the fluctuation conductivity $\sigma_1 - \sigma_n$ according to the three-dimensional (3D) LLL scheme.^{25,27} A very good scaling is achieved only with a linear choice of $T_c(B)$ line (equivalently B_{c2} line) for the temperature interval indicated in Fig. 4. The corresponding values are marked by arrows in Fig. 3. It is obvious that the values of B_{c2} obtained from the 3D LLL scaling are close to the points where the normal state seems to be reached, but not precisely there. This feature is due to the superconducting fluctuations, which appear also above the mean-field transition. By taking the deviation from the normal-state behavior as the onset of superconductivity, one selects, in fact, the point where the superconducting fluctuations start to exhibit a contribution noticeable above the noise level in the experimental curve.

The results of the present analysis are synthesized in Fig. 5. The full symbols represent the mean-field results B_{c2}^{MF} with vortices formed by a great number of Landau levels and having radius ξ_{MF} . The anisotropy ratio $\gamma_{MF} = \xi_{MF}^{ab} / \xi_{MF}^c \approx 2$ is practically temperature independent. The full lines in Fig. 5 are obtained from the 3D LLL scaling. These lines delineate the nucleation of vortices with the lowest Landau

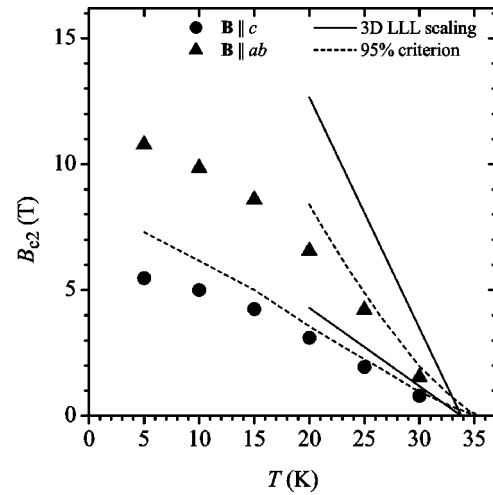


FIG. 5. The upper critical fields determined by various methods, B_{c2}^{MF} (symbols), B_{c2}^{GL} (full lines), and the values resulting from cutting the experimental curves (dashed lines).

level only. The field required for this nucleation is related to the Ginzburg-Landau coherence length $B_{c2}^{LLL} = \phi_0 / 2\pi \xi_{GL}^2$. The anisotropy ratio is $\gamma_{GL} = \xi_{GL}^{ab} / \xi_{GL}^c = 2.8$, and also temperature independent in the interval where the 3D LLL scaling could be applied.

We show by the dashed lines in Fig. 5 the results obtained by cutting the experimental curves of $1/2Q$ in Fig. 2 at 95% of the normal-state value. The line obtained in this way for $B_{c2}^{ab}(T)$ exhibits a positive curvature and, consequently, yields a temperature-dependent anisotropy ratio. Similar results have been obtained in other recent reports,⁸⁻¹² where various cutting criteria have been used rather than the scaling law. It is not possible to find a single cutting level that would mimic the 3D LLL scaling procedure. It appears that the cutting level should be changed from one experimental curve to another at a different temperature in a way that is, *a priori*, not known. Obviously, the effects of the superconducting fluctuations cannot be simply accounted for by a cutting procedure.

One may remark that the extrapolated B_{c2}^{LLL} lines in Fig. 5 point to $T_c = 33.8$ K, while the dashed lines based on the 95% cutting criterion reach 35.5 K. With a higher percentage for the cutting level, one could reach even higher temperatures. These values are in the fluctuation region above the true T_c defined as the temperature where ξ_{GL} diverges.

In conclusion, we have shown that in MgB₂, one can distinguish the mean-field coherence length in the mixed state, and the Ginzburg-Landau coherence length at the transition. The latter is found by considering the superconducting fluctuations and the proper scaling law of the measured physical quantity. We find the anisotropy ratios $\gamma_{MF} \approx 2$ and $\gamma_{GL} = 2.8$, both with no temperature dependences.

¹J. Nagamatsu, N. Nakagawa, T. Muranaka, Y. Zenitani, and J. Akimitsu, Nature (London) **410**, 63 (2001).

²C. Buzea and T. Yamashita, Supercond. Sci. Technol. **14**, R115 (2001).

³K.H.P. Kim, J.-H. Choi, C.U. Jung, P. Chowdhury, H.-S. Lee, M.-S. Park, H.-J. Kim, J.Y. Kim, Z.L. Du, E.-M. Choi, M.-S. Kim, W.N. Kang, S.-I. Lee, G.Y. Sung, and J.Y. Lee, Phys. Rev. B **65**, 100510 (2002).

- ⁴C. Ferdeghini, V. Ferrando, G. Grassano, W. Ramadan, E. Bellingeri, V. Braccini, D. Marre, M. Putti, P. Manfrinetti, A. Palenzona, F. Borgatti, R. Felici, and C. Aruta, *Physica C* **378-381**, 56 (2002).
- ⁵C. Ferdeghini, V. Braccini, M.R. Cimberle, D. Marre, P. Manfrinetti, V. Ferrando, M. Putti, and A. Palenzona, *Eur. Phys. J. B.* **30**, 147 (2002).
- ⁶M. Angst, R. Puzniak, A. Wisniewski, J. Jun, S.M. Kazakov, J. Karpinski, J. Roos, and H. Keller, *Phys. Rev. Lett.* **88**, 167004 (2002).
- ⁷K. Takahashi, T. Atsumi, N. Yamamoto, M. Xu, H. Kitazawa, and T. Ishida, *Phys. Rev. B* **66**, 012501 (2002).
- ⁸M. Angst, R. Puzniak, A. Wisniewski, J. Roos, H. Keller, and J. Karpinski, cond-mat/0206407 (unpublished).
- ⁹U. Welp, G. Karapetrov, W.K. Kwok, G.W. Crabtree, Ch. Marce-nat, L. Paulius, T. Klein, J. Marcus, K.H.P. Kim, C.U. Jung, H.-S. Lee, B. Kang, and S.-I. Lee, cond-mat/0203337 (unpublished).
- ¹⁰M. Zehetmayer, M. Eisterer, J. Jun, S.M. Kazakov, J. Karpinski, A. Wisniewski, and H.W. Weber, *Phys. Rev. B* **66**, 052505 (2002).
- ¹¹L. Lyard, P. Samuely, P. Szabo, T. Klein, C. Marce-nat, L. Paulius, K.H.P. Kim, C.U. Jung, H.-S. Lee, B. Kang, S. Choi, S.-I. Lee, J. Marcus, S. Blanchard, A.G.M. Jansen, U. Welp, G. Karapetrov, and W.K. Kwok, *Phys. Rev. B* **66**, 180502(R) (2002).
- ¹²A.V. Sologubenko, J. Jun, S.M. Kazakov, J. Karpinski, and H.R. Ott, *Phys. Rev. B* **65**, 180505(R) (2002).
- ¹³W.N. Kang, H.J. Kim, E.M. Choi, C.U. Jung, and S.-I. Lee, *Science* **292**, 1521 (2001).
- ¹⁴H.-J. Kim, W.N. Kang, E.-M. Choi, M.-S. Kim, K.H.P. Kim, and S.-I. Lee, *Phys. Rev. Lett.* **87**, 087002 (2001).
- ¹⁵M.-S. Kim, J.A. Skinta, T.R. Lemberger, W.N. Kang, H.-J. Kim, E.-M. Choi, and S.-I. Lee, *Phys. Rev. B* **66**, 064511 (2002).
- ¹⁶B.B. Jin, N. Klein, W.N. Kang, H.-J. Kim, E.-M. Choi, S.-I. Lee, T. Dahm, and K. Maki, *Phys. Rev. B* **66**, 104521 (2002).
- ¹⁷D.-N. Peligrad, B. Nebendahl, M. Mehring, A. Dulčić, M. Požek, and D. Paar, *Phys. Rev. B* **64**, 224504 (2001).
- ¹⁸A.A. Golubov, A. Brinkman, O.V. Dolgov, J. Kortus, and O. Jepsen, *Phys. Rev. B* **66**, 054524 (2002).
- ¹⁹A. Dulčić and M. Požek, *Physica C* **218**, 449 (1993).
- ²⁰M. Tinkham, *Introduction to Superconductivity* (McGraw-Hill, New York, 1975).
- ²¹Y. B. Kim and M. J. Stephen, in *Superconductivity*, edited by R. D. Parks (Dekker, New York, 1969), Vol. 2.
- ²²J. Owliaei, S. Sridhar, and J. Talvacchio, *Phys. Rev. Lett.* **69**, 3366 (1992).
- ²³I. Ukrainczyk and A. Dulčić, *Europhys. Lett.* **28**, 199 (1994).
- ²⁴M. Golosowsky, M. Tsindlekht, and D. Davidov, *Supercond. Sci. Technol.* **9**, 1 (1996).
- ²⁵S. Ullah and A.T. Dorsey, *Phys. Rev. B* **44**, 262 (1991).
- ²⁶U. Welp, S. Fleshler, W.K. Kwok, R.A. Klemm, V.M. Vinokur, J. Downey, B. Veal, and G.W. Crabtree, *Phys. Rev. Lett.* **67**, 3180 (1991).
- ²⁷I. Ukrainczyk and A. Dulčić, *Phys. Rev. B* **51**, 6788 (1995).